Loss of clusterin shifts amyloid deposition to the cerebrovasculature via disruption of perivascular drainage pathways

Aleksandra M. Wojtas[a,b], Silvia S. Kang[a], Benjamin M. Olley[c], Maureen Gatherer[c], Mitsuru Shinohara[a], Patricia A. Lozano[a], Chia-Chen Liu[a], Aishe Kurti[a], Kelsey E. Baker[a], Dennis W. Dickson[a,b], Mei Yue[a], Leonard Petrucelli[a], Guojun Bu[a,b], Roxana O. Carare[c], and John D. Fryer[a,b,1]

[a]Department of Neuroscience, Mayo Clinic, Jacksonville, FL 32224; [b]Neurobiology of Disease Graduate Program, Mayo Clinic Graduate School of Biomedical Sciences, Jacksonville, FL 32224; and [c]Faculty of Medicine, University of Southampton, Southampton General Hospital, Southampton SO16 6YD, United Kingdom

Edited by Gregory A. Petsko, Weill Cornell Medical College, New York, NY, and approved June 21, 2017 (received for review January 20, 2017)

Alzheimer's disease (AD) is characterized by amyloid-β (Aβ) peptide deposition in brain parenchyma as plaques and in cerebral blood vessels as cerebral amyloid angiopathy (CAA). CAA deposition leads to several clinical complications, including intracerebral hemorrhage. The underlying molecular mechanisms that regulate plaque and CAA deposition in the vast majority of sporadic AD patients remain unclear. The clusterin (*CLU*) gene is genetically associated with AD and CLU has been shown to alter aggregation, toxicity, and blood–brain barrier transport of Aβ, suggesting it might play a key role in regulating the balance between Aβ deposition and clearance in both brain and blood vessels. Here, we investigated the effect of CLU on Aβ pathology using the amyloid precursor protein/presenilin 1 (APP/PS1) mouse model of AD amyloidosis on a $Clu^{+/+}$ or $Clu^{-/-}$ background. We found a marked decrease in plaque deposition in the brain parenchyma but an equally striking increase in CAA within the cerebrovasculature of APP/PS1;$Clu^{-/-}$ mice. Surprisingly, despite the several-fold increase in CAA levels, APP/PS1;$Clu^{-/-}$ mice had significantly less hemorrhage and inflammation. Mice lacking CLU had impaired clearance of Aβ in vivo and exogenously added CLU significantly prevented Aβ binding to isolated vessels ex vivo. These findings suggest that in the absence of CLU, Aβ clearance shifts to perivascular drainage pathways, resulting in fewer parenchymal plaques but more CAA because of loss of CLU chaperone activity, complicating the potential therapeutic targeting of CLU for AD.

clusterin | Alzheimer's disease | cerebral amyloid angiopathy | Aβ | hemorrhage

Alzheimer's disease (AD) is the most common form of age-related dementia and represents a major health problem in the growing population of elderly people in developed countries (1). AD is characterized by pathological accumulation of tau as neurofibrillary tangles and deposition of toxic aggregates of amyloid-β (Aβ) peptide as fibrillar and diffuse plaques, resulting from the proteolytic cleavage of amyloid precursor protein (APP) by β- and γ-secretases (2–6). Additionally, Aβ can accumulate within the cerebral blood vessel walls, termed cerebral amyloid angiopathy (CAA). CAA is observed in the vast majority of AD patients (7–9), with Aβ deposition typically occurring in leptomeningeal vessels and penetrating arterioles (10). Several clinical complications arise from CAA, among which intracerebral hemorrhage is the most devastating (11). Additionally, familial forms of CAA arise from mutations within the Aβ coding region, resulting in enhanced Aβ aggregation in the basement membrane of the cerebrovasculature (12–15).

Rare forms of AD also exist from mutations in APP (16, 17) and other causative genes (18–20), leading to accelerated Aβ production and deposition, predominantly in the form of $Aβ_{42}$ (21, 22). However, it is still unclear what drives Aβ deposition in the more common sporadic form of AD. Growing evidence suggests that disruption of Aβ clearance mechanisms from the brain contributes to its accumulation, ultimately initiating the pathogenic cascade in AD (23). It has been shown that CAA can be induced by the failure of the perivascular drainage pathway to clear Aβ from the brain along cerebrovascular basement membranes (24). We have discovered several factors involved in perivascular drainage of Aβ, including apolipoprotein E (ApoE), aging, and high-fat diet (25–27). Therefore, uncovering additional factors that contribute to Aβ clearance by any means is critical to further our understanding of how Aβ plaque and CAA levels are regulated.

Clusterin (CLU), also known as apolipoprotein J (apoJ), is a multifaceted protein that regulates a broad range of biological processes, including lipid metabolism (28–30), apoptosis (31), spermatogenesis (32), and aggregation and adhesion of cells (33). The single CLU gene, located on chromosome 8 in humans (34, 35), encodes a 70- to 80-kDa highly glycosylated protein that is cleaved to form α- and β-subunits linked together by disulfide bonds during maturation (36, 37). With a central role in scavenging and survival (38, 39), the secreted form of CLU is a prominent chaperone in extracellular compartments (37). However, it has previously been reported that nuclear forms of CLU also exist from alternative splicing omitting exon 2 or translation from an alternative ATG start codon, although this is unique to the human transcript. Notably, nuclear CLU has been shown to trigger apoptosis in the cells under pathological conditions (40, 41).

Significance

Deposition of amyloid-β (Aβ) peptide in the form of parenchymal plaques and Aβ accumulation in the walls of cerebral vessels as cerebral amyloid angiopathy (CAA) are pathological hallmarks of Alzheimer's disease (AD). The clusterin (*CLU*) gene, which confers AD risk, is associated with amyloid deposition. Here we show that loss of CLU promotes cerebrovascular CAA, yet significantly reduces the amount of parenchymal plaques by altering perivascular drainage of Aβ in the APP/PS1 mouse model of AD. The absence of CLU in these mice is associated with a lower number of hemorrhages and a decrease in inflammation. These results suggest that CLU functions as a major Aβ chaperone to maintain Aβ solubility along interstitial fluid drainage pathways and prevent CAA formation.

Author contributions: J.D.F. designed research; A.M.W., S.S.K., B.M.O., M.G., M.S., P.A.L., C.-C.L., A.K., K.E.B., M.Y., and J.D.F. performed research; D.W.D., L.P., G.B., R.O.C., and J.D.F. contributed new reagents/analytic tools; A.M.W., S.S.K., M.G., L.P., G.B., R.O.C., and J.D.F. analyzed data; and A.M.W. and J.D.F. wrote the paper.

The authors declare no conflict of interest.

This article is a PNAS Direct Submission.

Freely available online through the PNAS open access option.

[1]To whom correspondence should be addressed. Email: Fryer.John@mayo.edu.

This article contains supporting information online at www.pnas.org/lookup/suppl/doi:10.1073/pnas.1701137114/-/DCSupplemental.

CLU is ubiquitously expressed in most mammalian tissues (29, 42–44), with the highest expression level in the CNS (45–47). For over two decades the ε4 allele of *APOE* has been recognized as a major risk factor for both AD and CAA development (48, 49). However, the role of CLU, another abundantly expressed apolipoprotein in the brain (50), in Aβ pathology has received significantly less attention. Importantly, the levels of CLU have been found to be significantly elevated in AD patients compared with nondemented elderly individuals (51). Moreover, in vitro studies have shown that CLU directly interacts with Aβ (52) and facilitates the formation of toxic Aβ fibrils (53, 54). Such a role of CLU in amyloid pathology has been supported by multiple in vivo studies showing a profound effect of CLU on Aβ aggregation and toxicity (55, 56), as well as Aβ transport across the blood–brain barrier (BBB) (57–59).

In addition to functional studies supporting the role of CLU in AD, genome-wide association studies (60–63) have previously shown that genetic allelic variance in *CLU* SNPs are significantly associated with AD risk. More recently, rare *CLU* variants associated with AD have also been identified (64). Although a previous study using a transgenic mouse model of AD (PDAPP model) investigated the role of CLU in amyloid plaque formation, the effect of CLU on Aβ metabolism and deposition in cerebral vessels was not examined (56). Here, we used the well-characterized APP/presenilin 1 (PS1) mouse model of AD amyloidosis crossed to *Clu* knockout ($Clu^{-/-}$) mice on a pure C57BL/6J background and conducted comprehensive histological and biochemical analyses.

Our findings have demonstrated that loss of CLU led to abundant CAA but simultaneously reduced brain parenchymal amyloid deposits. Despite the dramatic increase in CAA, the APP/PS1;$Clu^{-/-}$ mice presented with a significantly lower number of spontaneous hemorrhages and an overall decrease in inflammation and neuritic dystrophy compared with APP/PS1;$Clu^{+/+}$ littermates. Importantly, we have provided in vivo evidence that loss of CLU is sufficient to alter the efficiency of the Aβ clearance from the brain. Finally, the presence of exogenous CLU decreased the amount of $A\beta_{40}$ and $A\beta_{42}$ associated with cerebrovasculature in ex vivo binding experiments, suggesting that in the absence of CLU the clearance of Aβ shifts to more perivascular drainage but results in the deposition of amyloid in the vessel walls as CAA, because of loss of CLU chaperone function. Taking these data together, this study suggests a novel role for CLU in mediating perivascular clearance of Aβ from the brain but also indicates that therapeutic targeting of CLU might unintentionally shift pathology to CAA.

Results

CLU Colocalizes with Plaques and CAA and CLU Expression Determines Amyloid Distribution During Pathological Accumulation of Aβ. To examine the impact of CLU on amyloid pathology, we first investigated the pattern of CLU colocalization with Aβ deposits in brain parenchyma and cerebrovasculature in APP/PS1 transgenic mice (65). In this mouse model there is rapid Aβ accumulation in the brain and development of CAA-associated hemorrhage (66). CLU immunostaining with the Congo red derivative X-34 counterstaining to label fibrillar amyloid revealed intense labeling of CLU with a "halo-like" appearance surrounding amyloid plaques in the brain parenchyma (Fig. 1*A*). CLU also extensively colocalized to Aβ deposits in cerebral blood vessels in APP/PS1 mice (Fig. 1*A*). In addition, CLU showed association with Aβ deposits

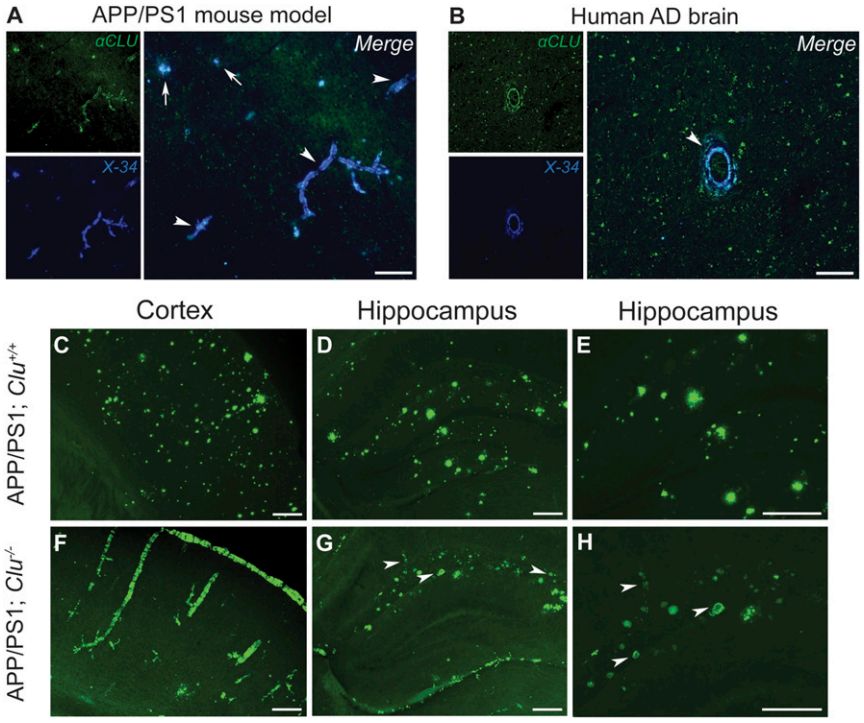

Fig. 1. CLU expression influences Aβ pathology associated with AD in cortex and hippocampus of 12-mo-old APP/PS1 mice. (*A* and *B*) CLU-colocalization with amyloid in brain parenchyma and cerebrovasculature in the APP/PS1 mouse model and in human AD brain tissue. X-34 was used to label fibrillar amyloid. (Scale bars, 50 μm.) (*A*) Representative brain section from APP/PS1 mouse showing halo-like colocalization of CLU (green) with amyloid plaques (blue) and complete colocalization with CAA (blue). (*B*) Representative brain section from patient with CAA showing colocalization of CLU with amyloid in cerebral vessel. Arrows indicate amyloid plaques and arrowheads indicate CAA. (*C–E*) APP/PS1;$Clu^{+/+}$ mice had abundant amyloid plaque pathology by 12 mo of age in the cortex and hippocampus. (*F–H*) However, APP/PS1;$Clu^{-/-}$ mice had a striking reduction in the amount of amyloid plaques in brain parenchyma and an increase in the amount of CAA in the cortex and hippocampus. (*G–H*) Arrowheads indicate Aβ deposits in small vessels in the hippocampus of APP/PS1;$Clu^{-/-}$, rarely present in APP/PS1;$Clu^{+/+}$ mice. (*C–H*) Thioflavine-S was used to label fibrillary amyloid. (Scale bars, 100 μm.)

in human cortex from an AD case with complete colocalization with CAA (Fig. 1*B*).

We then set out to determine whether changes in CLU levels influenced Aβ accumulation in the brain. We bred APP/PS1 mice onto a *Clu*$^{+/+}$ or a *Clu*$^{-/-}$ background (littermates on C57Bl6/J background strain) and harvested PBS-perfused brains at 6 and 12 mo of age. Immunohistochemical analysis of Aβ and thioflavine-S staining revealed that CLU loss did not impact the onset of Aβ deposition in the brain but substantially influenced where Aβ accumulated. Specifically, 6- and 12-mo-old APP/PS1;*Clu*$^{+/+}$ mice showed Aβ deposition mostly in the form of parenchymal plaques observed in the cortex (Fig. 1*C* and Fig. S1*A*) and hippocampus (Fig. 1 *D* and *E* and Fig. S1 *B* and *C*), whereas in APP/PS1;*Clu*$^{-/-}$ mice, Aβ was predominantly deposited in the cerebrovasculature as CAA (Fig. 1 *F*–*H* and Fig. S1 *D*–*F*). To more thoroughly analyze this dramatic shift in Aβ localization, we performed an unbiased stereological quantification of thioflavine-S^{+} deposits in brain parenchyma and cerebrovasculature in 6- and 12-mo-old mice (Fig. 2 and Fig. S2). We observed a highly significant reduction in the amount of thioflavine-S^{+} plaques in 6-mo-old APP/PS1;*Clu*$^{-/-}$ mice in the cortex ($P < 0.0001$) (Fig. S2*A*) and hippocampus ($P < 0.05$) (Fig. S2*A*) compared with control APP/PS1;*Clu*$^{+/+}$ littermates. The absence of CLU also caused an increase in thioflavine-S^{+} Aβ accumulation in leptomeningeal vessels ($P < 0.01$ in the cortex and $P < 0.05$ in the hippocampus) (Fig. S2*B*) and penetrating arterioles ($P < 0.05$ in the cortex and hippocampus) (Fig. S2*C*) at 6 mo of age. Similarly, 12-mo-old APP/PS1;*Clu*$^{-/-}$ mice also showed reduced thioflavine-S^{+} deposits in parenchymal plaques ($P < 0.0001$ in the cortex and hippocampus) (Fig. 2*A*) and increased CAA in leptomeningeal vessels of the cortex ($P = 0.062$) (Fig. 2*B*) and hippocampus ($P < 0.01$) (Fig. 2*B*) and penetrating arterioles ($P < 0.001$ in the cortex and $P < 0.05$ in the hippocampus) (Fig. 2*C*). In addition, the ratio of CAA to amyloid plaques was significantly increased in these brain regions in 12-mo-old APP/PS1;*Clu*$^{-/-}$ mice compared with APP/PS1;*Clu*$^{+/+}$ mice (Fig. 2*D*). Quantitatively, we observed a 40-fold and 6-fold increase in the ratio of CAA to parenchymal amyloid load in the cortex ($P < 0.0001$) and hippocampus ($P < 0.0001$), respectively, of 12-mo-old animals (Fig. 2*D*).

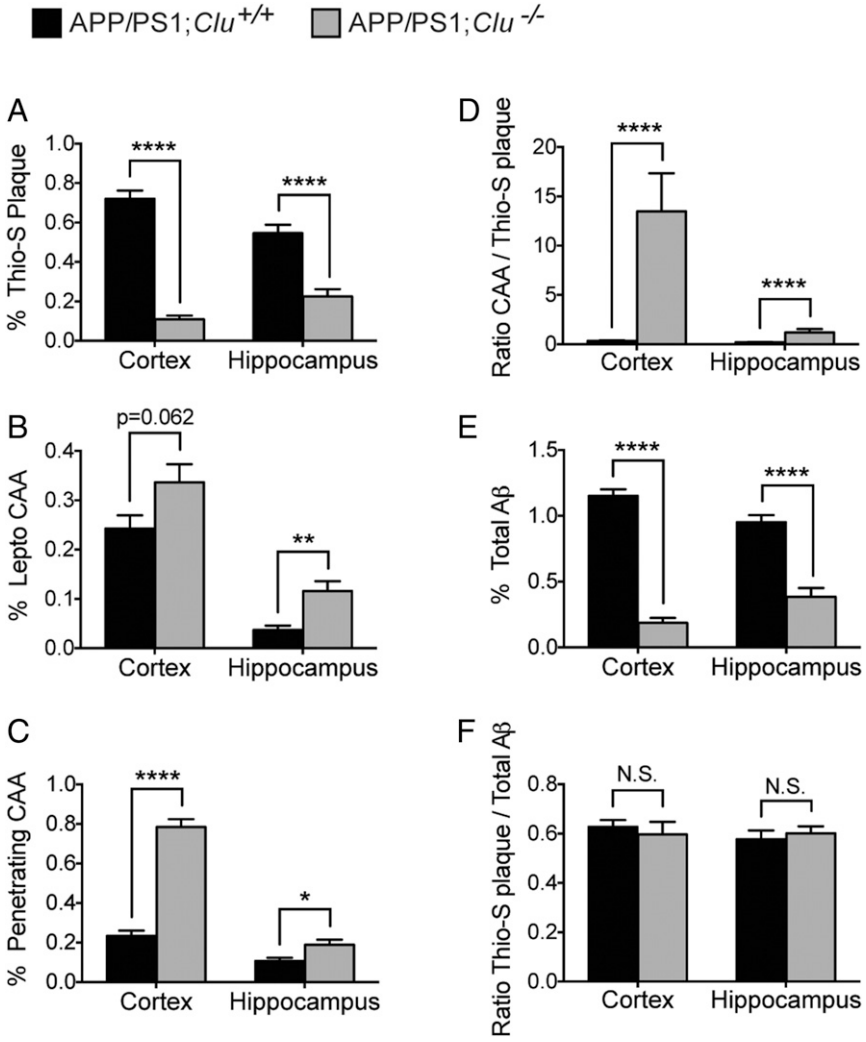

Fig. 2. Stereological quantification of amyloid deposition in brain parenchyma and cerebrovasculature in 12-mo-old APP/PS1 mice. (*A*) Twelve-month-old APP/PS1;*Clu*$^{-/-}$ mice had a significant decrease in the amount of amyloid plaques in cortex and hippocampus. (*B*) Significant increase in amyloid in leptomeningeal vessels and (*C*) penetrating arterioles was observed in the absence of CLU in cortex and hippocampus. (*D*) The ratio of CAA to thioflavine-S^{+} plaques was significantly increased in 12-mo-old APP/PS1;*Clu*$^{-/-}$ mice. (*E*) Twelve-month-old APP/PS1;*Clu*$^{-/-}$ mice also showed a decrease in the amount of total Aβ in the brain parenchyma in cortex and hippocampus. (*F*) The ratio of thioflavine-S^{+} amyloid plaques to total Aβ was not different between CLU genotypes in the cortex and hippocampus. Thioflavine-S (thio-S) was used to visualize fibrillar amyloid. $n = 11$–13 mice per group. For each animal three brain sections were analyzed. Data are presented as mean ± SEM and analyzed by Mann–Whitney test; *$P < 0.05$, **$P < 0.01$, ****$P < 0.0001$, N.S., not significant.

Similarly, at 6 mo of age, the ratio of CAA to amyloid plaques was a 50-fold increase in the cortex ($P < 0.0001$) and 5-fold increase in the hippocampus ($P < 0.01$) (Fig. S2*D*). Numerous small vessels of the hippocampus were thioflavine-S$^+$ in APP/PS1;*Clu*$^{-/-}$ mice (Fig. 1 *G* and *H* and Fig. S1 *E* and *F*), a feature rarely seen in this APP/PS1 model.

Given that Aβ peptide accumulates in the brain in the form of fibrillar (thioflavine-S$^+$) and diffuse (thioflavine-S$^-$) plaques, we next examined the total amount of Aβ in the same animal cohort by Aβ immunostaining and stereological quantification. We observed a significant decrease in total Aβ plaque levels in 6- ($P < 0.0001$ in the cortex and $P < 0.05$ in the hippocampus) (Fig. S2*E*) and 12-mo-old ($P < 0.0001$) (Fig. 2*E*) APP/PS1;*Clu*$^{-/-}$ mice compared with APP/PS1;*Clu*$^{+/+}$ littermates. Additionally, the ratio of fibrillar plaques to total Aβ did not differ between CLU genotypes (Fig. 2*F* and Fig. S2*F*), with the exception of the cortical region of 6-mo-old animals, which showed a significant reduction in this ratio in APP/PS1;*Clu*$^{-/-}$ mice in relation to APP/PS1;*Clu*$^{+/+}$ mice ($P < 0.0001$) (Fig. S2*F*). Finally, we evaluated sex-dependent effects of CLU on amyloid pathology in 6- and 12-mo-old mice (Figs. S3 and S4). We observed significant differences in amyloid plaque formation (Figs. S3*E* and S4 *A* and *E*) and CAA in penetrating vessels (Figs. S3*G* and S4 *C* and *G*) in 6- and 12-mo-old animals, with females having significantly more Aβ deposition in brain parenchyma and vasculature, suggesting a sex-associated increase in the severity of pathological presentation.

CLU Expression Alters Soluble and Insoluble Aβ Levels. Because CLU expression significantly impacts where Aβ deposits in the brain, we next examined whether the CLU genotype alters the levels of extractable forms of Aβ. ELISA was used to analyze insoluble (guanidine-HCl fraction, GDN) as well as TBS-soluble and detergent soluble (TBS with Trition X-100, TBS-X) forms of $A\beta_{40}$ and $A\beta_{42}$ from the cortex and hippocampus of 6- and 12-mo-old APP/PS1;*Clu*$^{+/+}$ and APP/PS1;*Clu*$^{-/-}$ mice (Fig. 3 and Fig. S5). In both APP/PS1;*Clu*$^{+/+}$ and APP/PS1;*Clu*$^{-/-}$ mice, substantially higher concentrations of $A\beta_{40}$ and $A\beta_{42}$ were found in the insoluble fraction relative to soluble Aβ forms within each genotype (Fig. 3 and Fig. S5), reflecting that the majority of Aβ is deposited as insoluble parenchymal plaques and CAA, respectively. Relative to controls, APP/PS1;*Clu*$^{-/-}$ mice showed significantly lower levels of $A\beta_{40}$ and $A\beta_{42}$ in the GDN fraction from the cortex at 6 and 12 mo of age ($P < 0.0001$) (Fig. 3*A* and Fig. S5*A*) and $A\beta_{42}$ from the hippocampus at 6 and 12 mo of age ($P < 0.01$ and $P < 0.05$) (Fig. 3*D* and Fig. S5*D*). Hippocampal levels of insoluble $A\beta_{40}$ were not statistically different between CLU genotypes (Fig. 3*D* and Fig. S5*D*). Similarly, TBS and TBS-X soluble fractions showed dramatic reduction of $A\beta_{40}$ and $A\beta_{42}$ levels in the cortex of 6- [$P < 0.01$ and $P < 0.0001$ (Fig. S5*B*) and $P < 0.0001$ (Fig. S5*C*)] and 12-mo-old [$P < 0.0001$ (Fig. 3*B*) and $P < 0.0001$ (Fig. 3C)] APP/PS1;*Clu*$^{-/-}$ mice in relation to control APP/PS1;*Clu*$^{+/+}$ mice. Additionally, we found that hippocampal concentrations of soluble $A\beta_{40}$ and $A\beta_{42}$ of 12-mo-old mice APP/PS1;*Clu*$^{-/-}$ [$P < 0.05$, $P < 0.0001$ (Fig. 3*E*) and $P < 0.01$, $P < 0.0001$ (Fig. 3*F*)] and $A\beta_{42}$ of 6-mo-old mice APP/PS1;*Clu*$^{-/-}$ [$P < 0.001$ (Fig. S5*E*) and $P < 0.01$ (Fig. S5*F*)] were significantly decreased relative to APP/PS1;*Clu*$^{+/+}$ controls. These data indicate that CLU expression alters the biochemical levels of Aβ deposition and are in agreement with the histological results.

Loss of CLU Significantly Reduces Parenchymal Plaque Load and Neuritic Dystrophy. Previous studies using AD mouse models have shown that severely dystrophic neurites surround fibrillar thioflavine-S$^+$ plaques in the brain parenchyma in a CLU-dependent manner (56). To determine whether the CLU genotype affects neuritic dystrophy, we performed double-labeling of brain sections with lysosomal-associated membrane protein 1, (Lamp1), to mark dystrophic neurites, and thioflavine-S, to define fibrillar plaques (Fig. 4 *A*–*C*

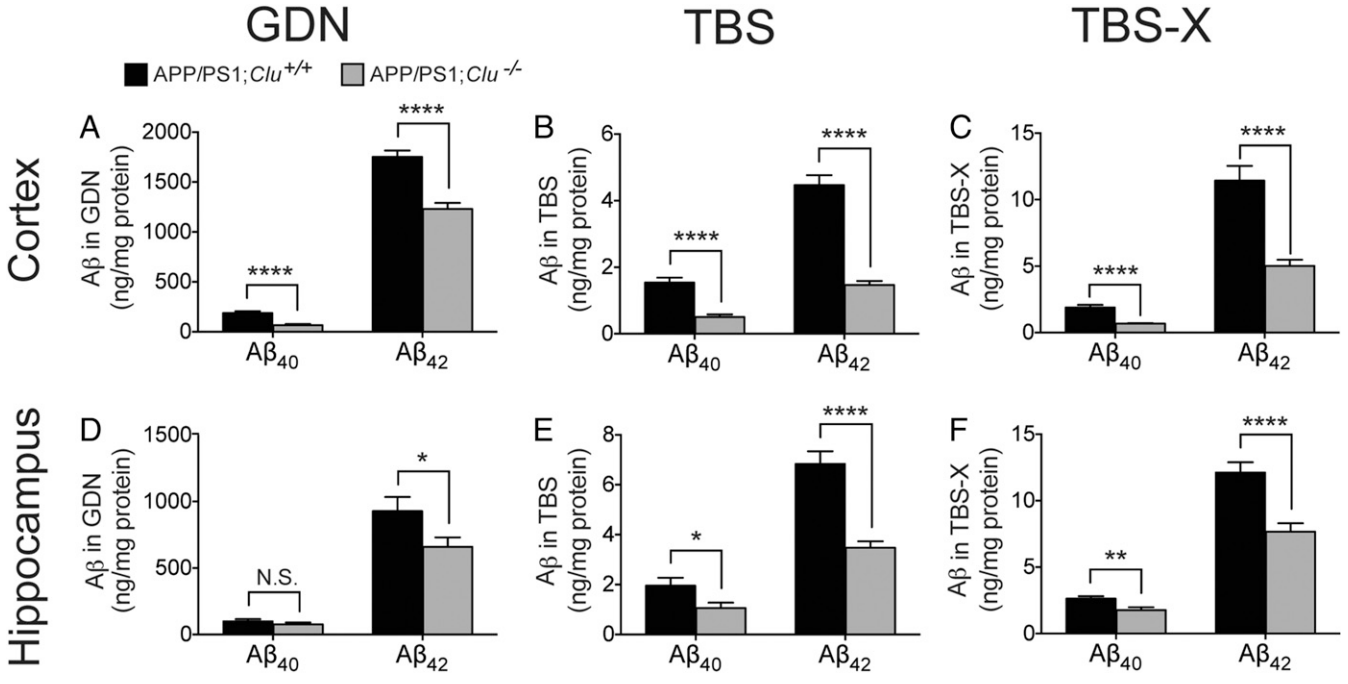

Fig. 3. CLU expression alters the levels of soluble and insoluble Aβ in cortex and hippocampus of 12-mo-old APP/PS1 mice. (*A*–*F*) Quantification of the Aβ levels in cortex and hippocampus of 12-mo-old APP/PS1 mice by ELISA. (*A*) APP/PS1;*Clu*$^{-/-}$ mice showed a significant decrease in the levels of insoluble $A\beta_{40}$ and $A\beta_{42}$ in cortex compared with control APP/PS1;*Clu*$^{+/+}$. (*B* and *C*) APP/PS1;*Clu*$^{-/-}$ mice had also reduced levels of (*B*) soluble and (*C*) detergent-soluble concentrations of $A\beta_{40}$ and $A\beta_{42}$ in cortex. (*D*) The levels of insoluble $A\beta_{42}$ but not $A\beta_{40}$ in the hippocampus of APP/PS1;*Clu*$^{-/-}$ mice were also reduced. (*E* and *F*) Concentration of (*E*) soluble and (*F*) detergent-soluble levels of $A\beta_{40}$ and $A\beta_{42}$ in hippocampus were decreased in the absence of CLU. $n = 15$–23 mice per group. Data are presented as mean ± SEM and analyzed by Mann–Whitney test; *$P < 0.05$, **$P < 0.01$, ****$P < 0.0001$, N.S., not significant.

and Fig. S6 *A–C*). As expected, we found numerous dystrophic neurites around parenchymal plaques in 6- (Fig. S6*A*) and 12-mo-old APP/PS1;$Clu^{+/+}$ mice (Fig. 4*A*) but none observed in proximity to CAA alone (Fig. 4*B* and Fig. S6*B*). APP/PS1;$Clu^{-/-}$ mice had a significant reduction in the amount of fibrillar thioflavine-S plaques and a corresponding reduction in the overall amount of neuritic dystrophy compared with APP/PS1;$Clu^{+/+}$ mice (Fig. 4 *B* and *D* and Fig. S6 *B* and *D*). However, although CLU has previously been reported to dissociate neuritic dystrophy from fibrillar amyloid plaques (56), we found no evidence of reduced neuritic dystrophy surrounding the few fibrillar thioflavin-S^+ plaques that were detected in APP/PS1;$Clu^{-/-}$ mice (Fig. 4*C* and Fig. S6*C*). The discrepancy between our results and previous reports may be because of differences in the APP transgenic model or the mixed genetic background of Demattos et al. (56), which also raises the possibility that other genetic modifiers are present that mediate the amyloid associated neuritic dystrophy.

Despite Increases in CAA, Absence of CLU Reduces Hemorrhage and Neuroinflammation Associated with Aβ Pathology. CAA is known to cause cerebral hemorrhage in AD patients (24). To examine if the elevated CAA observed in APP/PS1;$Clu^{-/-}$ mice was also associated with increased occurrence of cerebral hemorrhage, Prussian blue staining was conducted on 12-mo-old APP/PS1;$Clu^{+/+}$ and APP/PS1;$Clu^{-/-}$ mice ($n \geq 18$ sections per mouse spaced 300-μ apart). APP/PS1 mice predominantly develop microhemorrhages in the cortex and hippocampus because these two regions are the most severely affected by CAA. Despite the fact that they had substantially increased CAA, we found that APP/PS1;$Clu^{-/-}$ mice had significantly fewer spontaneous microhemorrhages compared with control APP/PS1;$Clu^{+/+}$ mice ($P < 0.05$) (Fig. 5*A*). When microhemorrhages were normalized to CAA load, we observed an even greater disparity between APP/PS1;$Clu^{+/+}$ and APP/PS1;$Clu^{-/-}$ mice ($P < 0.001$) (Fig. 5*B*).

Given that both parenchymal plaques and CAA are independently associated with neuroinflammation (67), we next investigated whether the CLU genotype had a differential effect on gliosis. Abundant astrogliosis was present around amyloid plaques in brain parenchyma of APP/PS1;$Clu^{+/+}$ mice (Fig. 5*C*). Although the absence of CLU resulted in a dramatic increase in CAA, the level of astrogliosis was significantly reduced when assessed at 12 mo of age in APP/PS1;$Clu^{-/-}$ mice (Fig. 5 *D* and *E*). Similarly, APP/PS1;$Clu^{-/-}$ mice had significantly decreased microgliosis compared with APP/PS1;$Clu^{+/+}$ mice (Fig. 5 *D* and *F*). Reactive astrocytes and microglia were not observed in proximity to CAA regardless of CLU genotype (Fig. 5*D*). To test whether CLU genotype also affected neuroinflammation at the molecular level, we profiled inflammatory cytokine transcripts, *Tnfα* and *Il6*, by real-time quantitative PCR. The levels of *Tnfα* and *Il6* were significantly increased in APP/PS1;$Clu^{+/+}$ compared with nontransgenic $Clu^{+/+}$ littermates, but these levels were significantly reduced to near baseline (nontransgenic levels) in APP/PS1;$Clu^{-/-}$ mice (Fig. 5 *G* and *H*). Taken together, these experiments demonstrate that the majority of inflammation in the presence of amyloid is because of parenchymal plaques rather than CAA, at least in the absence of CLU.

CLU Does Not Impact APP Processing or Cause Widespread Transcriptional Changes in Known Aβ Metabolism Pathways. The intriguing association between loss of CLU and dramatic increase in CAA led us to test whether CLU alters APP metabolism. We performed Western blot analysis to assess the level of full-length APP and soluble APPα (sAPPα) in brain homogenates of APP/PS1;$Clu^{+/+}$ and APP/PS1;$Clu^{-/-}$ mice (Fig. S7*A*). The CLU genotype did not alter APP and sAPPα expression levels, indicating that CLU does not grossly affect APP processing (Fig. S7 *B* and *C*).

A myriad of other factors besides APP processing could explain the shift in Aβ pathology from parenchymal plaques to

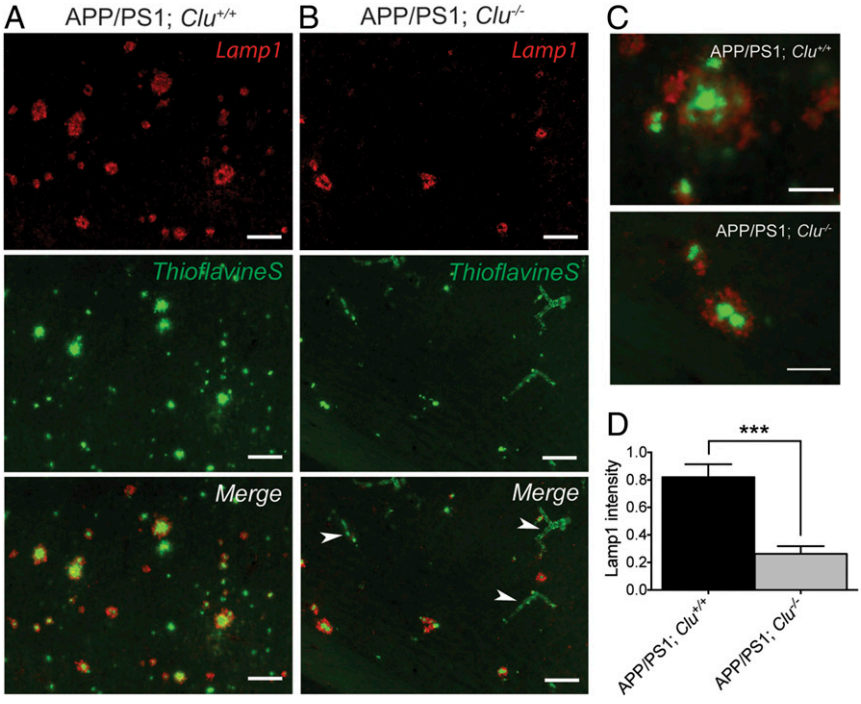

Fig. 4. Absence of CLU reduces the total amount of neuritic dystrophy in APP/PS1 mice. (*A*) In APP/PS1;$Clu^{+/+}$ mice all parenchymal plaques (green) were surrounded by dystrophic neurites (red) identified with Lamp1 antibody. (*B*) APP/PS1;$Clu^{-/-}$ mice had an overall reduction in the amount of parenchymal plaques and a concomitant reduction in total neuritic dystrophy. Arrowheads indicate CAA. (Scale bars in *A* and *B*, 50 μm.) (*C*) However, prominent neuritic dystrophy was seen around parenchymal plaques that do form in APP/PS1;$Clu^{-/-}$ mice. (Scale bars, 20 μm.) (*D*) Quantification of Lamp1 intensity in brain sections of 12-mo-old APP/PS1 mice. $n = 8–12$ mice per group. Data are presented as mean ± SEM and analyzed by Mann–Whitney test; ***$P < 0.001$.

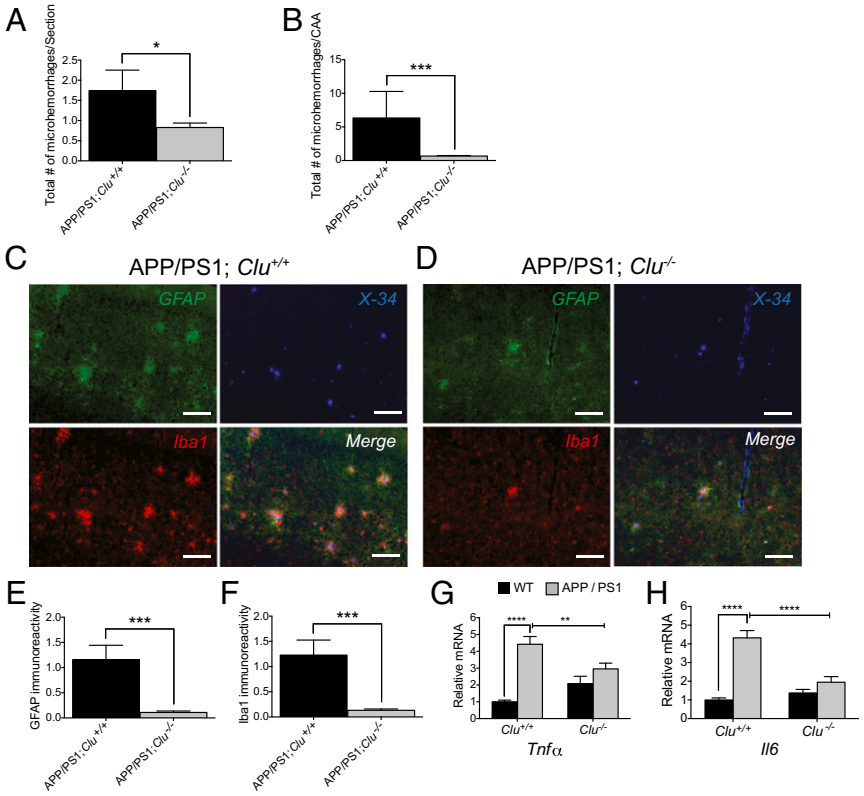

Fig. 5. The absence of CLU in APP/PS1 mice prevents hemorrhage and inflammation at the cellular and molecular level. (*A* and *B*) Quantification of CAA-associated hemorrhage in 12-mo-old APP/PS1 mice. (*A*) Despite the abundant increase in CAA, APP/PS1;$Clu^{-/-}$ mice had significantly reduced total number of microhemorrhages and (*B*) number of microhemorrhages normalized to CAA load compared with control APP/PS1;$Clu^{+/+}$ animals. $n = 11$–13 mice per group. For each animal, 18–21 brain sections were analyzed. Data are presented as mean ± SEM and analyzed by Mann–Whitney test; $^{*}P < 0.05$ and $^{***}P < 0.001$. (*C*) APP/PS1;$Clu^{+/+}$ mice had abundant astrogliosis (green) and microgliosis (red) surrounding amyloid plaques (blue). (*D*) Despite the dramatic increase in CAA in APP/PS1;$Clu^{-/-}$ mice, the overall level of gliosis was significantly reduced. (Scale bars in *C* and *D*, 50 μm.) (*E*) Quantification of astrogliosis showed the significant decrease in the number of reactive astrocytes in APP/PS1;$Clu^{-/-}$ mice compared with control. (*F*) Quantification of microgliosis showing reduction of reactive microglia in APP/PS1;$Clu^{-/-}$ mice compared with APP/PS1;$Clu^{+/+}$ animals. $n = 7$–11 mice per group. Data are presented as mean ± SEM and analyzed by Mann–Whitney test; $^{***}P < 0.001$. (*G* and *H*) APP/PS1;$Clu^{+/+}$ mice had increased levels of proinflammatory cytokines, such as *Tnfα* and *Il6*, compared with nontransgenic (nTg) $Clu^{+/+}$ animals. However, this increase in proinflammatory cytokines was significantly reduced in APP/PS1;$Clu^{-/-}$ mice. $n = 8$–10 mice per group. Data are presented as mean ± SEM and analyzed by two-way ANOVA with post hoc Tukey's test; $^{**}P < 0.01$, $^{****}P < 0.0001$.

CAA. We therefore sought to determine whether specific CLU-dependent changes occurred in the brain transcriptome that might explain this shift in pathology. To identify differentially expressed transcripts between CLU genotypes, we performed an RNAseq transcriptomic study of whole-brain tissue from 6-mo-old $Clu^{+/+}$ and $Clu^{-/-}$ mice ($n = 4$ per genotype). However, this analysis yielded only four protein-coding transcripts that were differentially expressed after false-discovery rate correction between $Clu^{+/+}$ and $Clu^{-/-}$ mice, including *Clu* itself, *Slc25a37*, *Hprt*, and *Frem1* (Table S1). No significant changes were found in other AD genes, such as *Apoe*, *Bin1*, *Abca7*, *Picalm*, *Cd33*, *Cd2ap*, or any of the several putative Aβ degrading enzymes (Table S2). It has previously been shown that overexpression of *Tgfb1* in APP transgenic mice results in a shift in Aβ pathology from parenchyma to vessels (68), but our transcriptome study did not show any significant changes in *Tgfb1* or the TGF-β pathway in general. These findings suggest that CLU-deficiency itself does not significantly impact the whole-brain transcriptome and that the effects seen on Aβ deposition are likely direct in nature.

CLU Alters Aβ Clearance Pathway and Prevents ex Vivo Binding of Aβ to Isolated Cerebrovasculature. To gain insight into the possible mechanism underlying the dramatic shift in the Aβ deposition from parenchyma to cerebrovasculature in APP/PS1;$Clu^{-/-}$ mice, we used in vivo microdialysis (Fig. 6 *A*–*C*). Because soluble Aβ in the interstitial fluid (ISF) has been shown to correlate with Aβ deposited in the brain parenchyma (69), we measured the hippocampal steady-state levels in 10-wk-old APP/PS1;$Clu^{+/+}$ and APP/PS1;$Clu^{-/-}$ mice. To determine whether CLU genotype had a differential effect on Aβ clearance, we infused a potent γ-secretase inhibitor that rapidly blocked Aβ production, therefore allowing us to examine the half-life ($t_{1/2}$) of $Aβ_{40}$. The concentration of hippocampal $Aβ_{40}$, measured in ISF, gradually decreased over time, with APP/PS1;$Clu^{+/+}$ showing faster decline compared with APP/PS1;$Clu^{-/-}$ mice (Fig. 6*B*). Moreover the $t_{1/2}$ of ISF $Aβ_{40}$ was significantly longer in mice lacking CLU compared with control littermates ($P < 0.05$) (Fig. 6*C*). These results suggest that the loss of CLU may alter the clearance of soluble Aβ from the ISF.

Numerous studies have previously shown that $Aβ_{40}$ is predominantly present in vascular amyloid because of its more soluble nature (70, 71), whereas $Aβ_{42}$, a more fibrillogenic form of Aβ, is mainly found in parenchymal amyloid (72, 73). Therefore, the ratio of Aβ*40:42* seems to determine where Aβ deposits in the brain with higher Aβ*40:42* ratio predisposing the formation of CAA (74). In agreement with this hypothesis, we found a slight increase in the Aβ*40:42* ratio ($P = 0.057$) (Fig. 6*D*) in APP/PS1;$Clu^{-/-}$ mice compared with APP/PS1;$Clu^{+/+}$ mice.

Given that CAA and AD appear to result from a disruption of the perivascular drainage pathway (24, 75), we sought to investigate the potential role of CLU in the Aβ removal along the

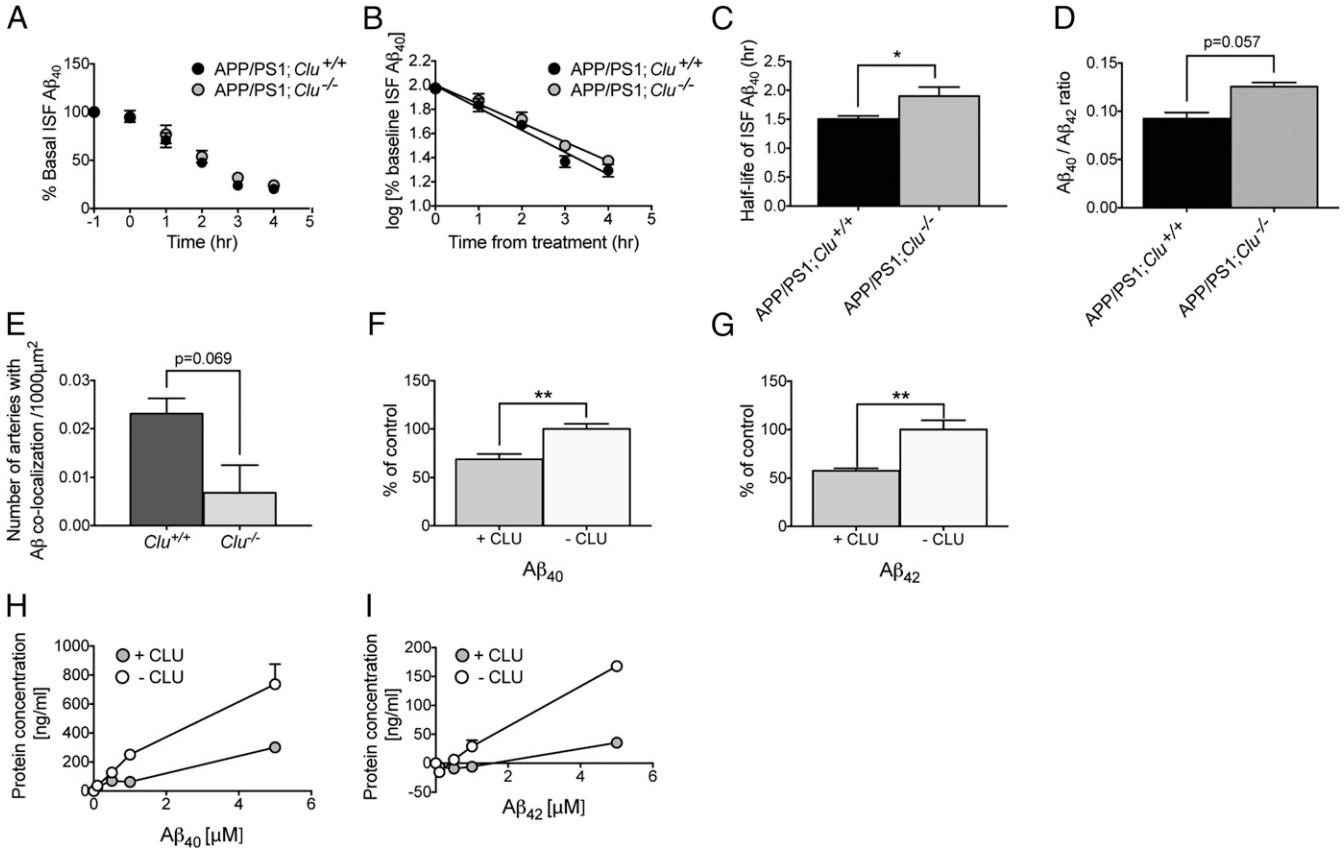

Fig. 6. CLU alters Aβ clearance and prevents binding of soluble Aβ to cerebrovasculature. (*A–C*) In vivo microdialysis to assess the Aβ metabolism in the hippocampus of 10-wk-old APP/PS1;$Clu^{+/+}$ and APP/PS1;$Clu^{-/-}$. (*A*) The concentration of $A\beta_{40}$ in ISF was measured as the basal level of Aβ. (*B*) The logarithm (log) of percentage baseline ISF $A\beta_{40}$ versus time was plotted after treatment of mice with a potent γ-secretase inhibitor. (*C*) The slope from the linear regressions from log (percent ISF $A\beta_{40}$) was used to assess the half-life of $A\beta_{40}$ elimination from the ISF. $n = 5–6$ mice per group. Data are presented as ± SEM and analyzed by Student's *t* test; $^*P < 0.05$. (*D*) The ratio of Aβ*40:42* was examined from 10-wk-old APP/PS1;$Clu^{+/+}$ and APP/PS1;$Clu^{-/-}$. (*E*) Quantification of the number of arteries with colocalization of fluorescently labeled human $A\beta_{40}$. Fewer arteries with Aβ colocalization were observed in $Clu^{-/-}$ mice compared with $Clu^{+/+}$ animals. (*F* and *G*) Exogenous (*F*) $A\beta_{40}$ and (*G*) $A\beta_{42}$ were applied to isolated cerebral vessels with and without exogenously added CLU and binding of Aβ was measured by ELISA. The addition of 1 μM exogenous CLU led to a significant reduction in the levels of (*F*) $A\beta_{40}$ and (*G*) $A\beta_{42}$ associated with cerebrovasculature. (*H* and *I*) Isolated vessels were treated with increasing concentrations of exogenous (*H*) $A\beta_{40}$ and (*I*) $A\beta_{42}$ in the absence and presence of increasing concentrations of CLU. CLU addition resulted in a decrease amount of (*H*) $A\beta_{40}$ and (*I*) $A\beta_{42}$ bound to cerebral vessels even at high Aβ concentrations. Data presented as ELISA replicates. $n = 3–4$ mice per group. Data are presented as ± SEM and analyzed by Student's *t* test; $^{**}P < 0.01$.

basement membrane of cerebral vessels. Therefore, we examined the pattern of distribution of fluorescently labeled human $A\beta_{40}$ following its intracerebral injection of 3-mo-old $Clu^{+/+}$ and $Clu^{-/-}$ mice, as we have previously described (25, 26). The difference in counts of arteries with Aβ colocalization between the injection site and 100-μm posterior was calculated as a measure of perivascular drainage 10 min after injection of fluorescently labeled $A\beta_{40}$. We detected fewer arteries with fluorescent Aβ localization in $Clu^{-/-}$ mice compared with control littermates ($P = 0.069$) (Fig. 6*E*), suggesting that perivascular drainage of Aβ might be compromised in the brains of $Clu^{-/-}$ animals.

These findings led us to evaluate whether there was a direct effect of CLU on CAA by measuring the ability of CLU to alter binding of Aβ to the cerebrovasculature in an ex vivo binding assay. To this end, we freshly isolated cerebral vessels using density-mediated separation to purify vessels from parenchymal components, as previously described (76). Vessels were then treated with exogenous human $A\beta_{40}$ or $A\beta_{42}$, in the presence or absence of exogenous CLU, then washed, lysed in GDN buffer, and Aβ levels were assessed by ELISA. We found that addition of exogenous CLU resulted in a significant reduction of the amount of $A\beta_{40}$ ($P < 0.01$) (Fig. 6*F*) and $A\beta_{42}$ ($P < 0.01$) (Fig. 6*G*) bound to isolated cerebral blood vessels compared with samples lacking exogenous CLU. A similar effect was observed when isolated cerebral vessels were treated with increasing concentrations of exogenous $A\beta_{40}$ or $A\beta_{42}$ in the presence of equally increasing concentrations of exogenous CLU (Fig. 6 *H* and *I*). The addition of exogenous CLU led to a dramatic decrease of the level of Aβ associated with the cerebrovasculature compared with vessels without CLU added, even when assessed at high Aβ concentrations. Taken together, these results suggest that in the absence of CLU, Aβ clearance shifts to perivascular drainage, resulting in decreased parenchymal amyloid but also in the aggregation and deposition in the cerebral blood vessels because of loss of CLU chaperone activity.

Discussion

In the present study, we investigated whether alterations in CLU expression affect amyloid-driven pathology. Using the APP/PS1 mouse model of AD amyloidosis, we showed that in sharp contrast to the abundant brain parenchmal amyloid plaque accumulation and minimal CAA observed in APP/PS1; $Clu^{+/+}$ mice, APP/PS1;$Clu^{-/-}$ mice had few parenchymal plaques but robust CAA, even when assessed at a young age. In addition, CLU loss resulted in substantial alterations of dynamic pools of soluble and insoluble Aβ. We further demonstrated that lack of CLU significantly reduced the number of

CAA-associated microhemorrhages, despite the fact that the APP/PS1;$Clu^{-/-}$ mice had a tremendous elevation in the amount of CAA. Our in vivo data also showed that APP/PS1;$Clu^{-/-}$ mice exhibited significantly less neuritic dystrophy and reduced cellular and molecular inflammation compared with APP/PS1;$Clu^{+/+}$ mice. Importantly, by using in vivo microdialysis, we provided evidence that CLU is involved in the elimination of Aβ from the brain. Consistent with this notion, intracerebral injections of $A\beta_{40}$ of young $Clu^{+/+}$ and $Clu^{-/-}$ mice resulted in a decreased number of arteries with fluorescently labeled $A\beta_{40}$, implying the disruption of perivascular drainage pathway in the absence of CLU. Finally, we identified that the presence of exogenously added CLU reduced binding of $A\beta_{40}$ and $A\beta_{42}$ to isolated cerebral vessels, suggesting that CLU impacts Aβ pathology in vessels by preventing it from binding and aggregating during ISF drainage.

Growing evidence suggests that CLU is an important player in Aβ deposition, fibrillogenesis, and clearance (53, 55–57). The in vivo consequences of CLU loss were previously assessed in the PDAPP mouse model of AD (55, 56). These seminal reports showed that absence of CLU was associated with a substantial reduction of fibrillar amyloid plaques but no change in total Aβ deposition in brain parenchyma. Our data are in agreement with the effect of CLU on fibrillar plaques but, in contrast, we found that loss of CLU also reduced total Aβ load.

One of the most striking phenotypes of CLU loss in our AD amyloidosis model was the shift in the localization of Aβ deposition from parenchymal plaques to CAA. Although DeMattos et al. (56) did not directly analyze CAA levels in their study, such an obvious pathology would have been readily noticed. Therefore, the differences in these studies likely reflect the different APP transgenic models used (PDAPP vs. APP/PS1) or the mixed genetic background of the PDAPP mouse model.

In light of increasing evidence that disruption of Aβ clearance mechanisms from the brain initiates the pathogenic cascade of AD (23), identifying factors that contribute to Aβ elimination is critical. Importantly, we showed that the loss of CLU is sufficient to reduce the efficiency of Aβ clearance in the hippocampus in our mouse model of AD amyloidosis. In agreement with this observation, we found an increased Aβ*40:42* ratio in APP/PS1;$Clu^{-/-}$ mice, possibly contributing to the shift of Aβ deposition between brain compartments. Given that $A\beta_{40}$ appears to mediate accumulation of amyloid in cerebral vessels (70, 71), whereas $A\beta_{42}$ is thought to be a predominant form present in the brain parenchyma (72, 73), Aβ*40:42* ratio might be an important factor in determining where Aβ deposits.

In fact, several lines of evidence have previously suggested that a high Aβ*40:42* ratio favors the development of CAA (74, 77). The APPDutch animal model, which recapitulates the characteristics of hereditary cerebral hemorrhage with amyloidosis- Dutch type (HCHWA-D) and shows Aβ accumulation predominantly in the cerebral vessels, appears to have a highly elevated Aβ*40:42* ratio compared with animals overexpressing human wild-type APP (77). In addition, it has been reported that Tg2576 mice expressing human ApoE4 develop CAA, which is also likely attributable to the higher ratio of Aβ*40:42* in these animals in relation to animals expressing endogenous murine ApoE (74). In contrast, a lower Aβ*40:42* ratio seems to promote amyloid deposition in brain parenchyma versus cerebrovasculature. It has been shown that APP mice harboring the "Indiana" mutation, which leads to the highly elevated levels of $A\beta_{42}$, have a reduction in Aβ*40:42* ratio, and therefore mainly parenchymal deposition of Aβ (78). This notion is further supported by observation that PDAPP mice lacking ApoE have an increased production of $A\beta_{42}$, which results in deposition of parenchymal amyloid with very minimal CAA (76).

Among numerous Aβ clearance pathways in the brain that have previously been described (57, 68, 79–84), perivascular drainage along basement membranes of cerebral arteries is one of the major routes for Aβ removal and its impairment leads to CAA formation (25, 26). We found a reduced number of arteries with colocalization of injected fluorescent Aβ in the basement membranes in $Clu^{-/-}$ mice compared with control littermates, suggesting the disruption of perivascular drainage of Aβ in the absence of CLU. Consistent with this notion, we found direct ex vivo evidence that CLU alters Aβ binding to isolated cerebral vessels, which might exacerbate development of CAA. Therefore, we propose that CLU facilitates Aβ clearance along ISF drainage pathways by preventing binding to cerebral vessels, possibly through the interactions with cerebrovascular basement membrane components. Thus, as a consequence of CLU loss, Aβ fibrils accumulate in the cerebral vessels and lead to CAA.

Interestingly, using unbiased proteomic analysis, we have recently demonstrated that the level of CLU protein is significantly elevated in human leptomeningeal arteries with CAA (85), suggesting the entrapment of the Aβ–CLU complex in the perivascular drainage pathways, or a compensatory up-regulation of CLU to clear Aβ.

Despite the evidence that loss of CLU leads to the accumulation of Aβ in the walls of cerebral vessels, possibly mediating the formation of CAA, we cannot rule out the possibility that other mechanisms also contribute to Aβ deposition in different brain compartments. Previous reports have demonstrated that the transport of soluble Aβ across the BBB can be facilitated via low-density lipoprotein receptor-related protein-1 (LRP1) (84). In addition, the low-density LRP2 has been previously shown to mediate the elimination of $A\beta_{42}$ from the brain. LRP2 is a receptor for CLU localized at the BBB and it has been suggested to be essential for the transport of the Aβ–CLU complex into circulation (57). It is possible that the absence of CLU also disrupts the Aβ transport across the BBB via LRP2, leading to the accumulation of Aβ within the walls of the cerebrovasculature. Although the BBB plays a significant role in the Aβ clearance, whether and to what extend BBB transporters contribute to the development of CAA in APP/PS1;$Clu^{-/-}$ mice is yet to be determined, although we found no evidence of altered transcript levels of *Lrp1*, *Lrp2*, or other members of the LDLR family in our RNAseq data.

Mounting evidence has demonstrated the strong association between CAA and cerebral hemorrhage in elderly individuals. Recurrent cerebral hemorrhage is also present in patients with hereditary cerebral hemorrhage with amyloidosis Icelandic type (HCHWA-I), however it is also frequently observed in individuals with sporadic CAA (86, 87). Several lines of evidence suggest that cerebral hemorrhage is caused by gradual smooth muscle cell degeneration in the walls of cerebral vessels, leading to their weakening and rupture (88). Spontaneous acute hemorrhage has also been linked to widespread Aβ deposition in leptomeningeal and cortical vessels in several transgenic mice. Winkler et al. showed that accumulation of Aβ is sufficient to give rise to recurrent hemorrhagic stroke in APP23 mice (89). Similar findings have been reported for other transgenic mouse models overexpressing human APP harboring various mutations, including Tg2576, PDAPP (76), TgSwDI (90), and APPDutch (77), which develop spontaneous hemorrhage in association with Aβ-laden vessels. Interestingly, the loss of ApoE in Tg2576 and PDAPP mice completely prevented CAA and hemorrhage, indicating that ApoE facilitates CAA and CAA-associated hemorrhage (76). Although CAA is a major risk factor for developing hemorrhage, we observed a significant decrease in the number of microhemorrhages in APP/PS1;$Clu^{-/-}$ mice compared with APP/PS1;$Clu^{+/+}$ animals. A possible explanation for this difference with previous studies could be that CLU expression alters the structure or amount of amyloid deposited in the walls of cerebrovasculature, causing their damage.

It is recognized that neuroinflammation is another component commonly observed in individuals with CAA (91). Similar to human studies, Herzig et al. have observed that an inflammatory response is associated with vascular amyloid and exists independently from amyloid plaques in APPDutch mice (77). Miao

et al. have shown that reactive astrocytes and activated microglia were present in vicinity of Aβ-laden vessels in Tg-SwDI transgenic mice (92). In addition, elevated levels of inflammatory cytokines, including IL-6 and IL-1β, were noted in these animals (92). Although these studies support an association of vascular amyloid with neuroinflammation, the majority of CAA in these models is weighted toward capillaries. Our data indicate that the cellular and molecular inflammation are more associated with parenchymal amyloid load rather than CAA. These observations raise the possibility that CAA, as seen in sporadic CAA, is not sufficient to cause neuroinflammation in APP/PS1 mice or that the combination of CAA and CLU expression is critical for induction of inflammatory response. Additional studies are needed to further address this issue.

Given the role of CLU in Aβ accumulation, transport, and toxicity, and its strong genetic association with AD, we aimed to elucidate how CLU affects Aβ pathology and discovered a role in the pathophysiology of both parenchymal plaque formation as well as CAA. Future studies are crucial to gain a detailed view of additional mechanisms underlying the role of CLU in CAA and to better understand specific events leading to pathogenesis of AD and CAA. This could allow optimization of therapeutic strategies to limit Aβ deposition in brain parenchyma and cerebrovasculature. Therapeutics that intentionally or unintentionally decrease the levels of CLU may result in an unwanted shift of Aβ pathology to CAA, although our data indicate that the brain may be more tolerant of amyloid in the cerebrovasculature than in the parenchyma.

Materials and Methods

Animals. APP/PS1 mice bearing a double-mutation APPswe/PS1ΔE9 were used (65). All studies were done in accordance with *National Institutes of Health Guide for the Care and Use of Laboratory Animals* (93) under an approved protocol from the Mayo Clinic Institutional Animal Care and Use Committee. De-identified postmortem, pathologically confirmed AD brain tissue were obtained through the Mayo Clinic Brain Bank for neurodegenerative diseases, whose operating procedures are approved by the Mayo Institutional Review Board.

Histopathological Analyses. PBS-perfused brains from APP/PS1;$Clu^{+/+}$ and APP/PS1;$Clu^{-/-}$ mice were used and analyzed using a Zeiss AxioImager.Z1/ApoTome microscope. Aβ pathology was quantified, as previously described (76).

Biochemical Analyses. Cortex and hippocampus were dissected from APP/PS1;$Clu^{+/+}$ and APP/PS1;$Clu^{-/-}$ PBS-perfused brains. Separate extraction for each condition was used. $A\beta_{40}$ and $A\beta_{42}$ levels were assessed by ELISAs. To examine APP processing, the cortices of APP/PS1;$Clu^{+/+}$ and APP/PS1;$Clu^{-/-}$ mice were used. Total RNA was isolated using a Total Aurum RNA isolation kit. Random-primed reverse transcription was performed. All samples were run on an ABI 7900 HT Fast Real-Time PCR instrument.

In Vivo Clearance. In vivo microdialysis in APP/PS1;$Clu^{+/+}$ and APP/PS1;$Clu^{-/-}$ mice was performed, as described previously (69, 94). Perivascular drainage was quantified in $Clu^{+/+}$ and $Clu^{-/-}$ mice, as described previously (25).

Aβ Binding to Cerebrovasculature. Cerebral vessels were isolated from C57BL/6J mice, as described previously (76). Vessels were treated with $A\beta_{40}$ or $A\beta_{42}$ with or without CLU. The Aβ binding to vasculature was assessed by ELISA.

Statistical Analyses. For all statistical analyses GraphPad Prism 5.04 software was used. For additional descriptions of methods, please see *SI Materials and Methods*.

ACKNOWLEDGMENTS. J.D.F. was supported by the Mayo Foundation, the GHR Foundation, the Mayo Clinic Center for Individualized Medicine, a Mayo Clinic Gerstner Family Career Development Award, the Ed and Ethel Moore Alzheimer's Disease Research Program of Florida Department of Health (6AZ06), the Gilmer Family Foundation, Alzheimer's Association NIRP-12-25928, and NIH Grants NS094137, AG047327, and AG049992. S.S.K. was supported by The Robert and Clarice Smith and Abigail Van Buren Alzheimer's Disease Research Program Fellowship, the Mayo Clinic Program on Synaptic Biology and Memory, and NIH Grant MH103632. G.B. was supported by NIH Grants AG027924, AG035355, and NS074969.

1. Alzheimer's Association (2014) 2014 Alzheimer's disease facts and figures. *Alzheimers Dement* 10:e47–e92.
2. Vassar R, et al. (1999) Beta-secretase cleavage of Alzheimer's amyloid precursor protein by the transmembrane aspartic protease BACE. *Science* 286:735–741.
3. Kimberly WT, et al. (2003) Gamma-secretase is a membrane protein complex comprised of presenilin, nicastrin, Aph-1, and Pen-2. *Proc Natl Acad Sci USA* 100:6382–6387.
4. Glenner GG, Wong CW (1984) Alzheimer's disease: Initial report of the purification and characterization of a novel cerebrovascular amyloid protein. *Biochem Biophys Res Commun* 120:885–890.
5. Grundke-Iqbal I, et al. (1986) Microtubule-associated protein tau. A component of Alzheimer paired helical filaments. *J Biol Chem* 261:6084–6089.
6. Walsh DM, Selkoe DJ (2004) Deciphering the molecular basis of memory failure in Alzheimer's disease. *Neuron* 44:181–193.
7. Vinters HV (1987) Cerebral amyloid angiopathy. A critical review. *Stroke* 18:311–324.
8. Jellinger KA (2002) Alzheimer disease and cerebrovascular pathology: An update. *J Neural Transm (Vienna)* 109:813–836.
9. Roher AE, et al. (2003) Cortical and leptomeningeal cerebrovascular amyloid and white matter pathology in Alzheimer's disease. *Mol Med* 9:112–122.
10. Revesz T, et al. (2002) Sporadic and familial cerebral amyloid angiopathies. *Brain Pathol* 12:343–357.
11. Yamada M (2015) Cerebral amyloid angiopathy: Emerging concepts. *J Stroke* 17:17–30.
12. Levy E, et al. (1990) Mutation of the Alzheimer's disease amyloid gene in hereditary cerebral hemorrhage, Dutch type. *Science* 248:1124–1126.
13. Maat-Schieman M, Roos R, van Duinen S (2005) Hereditary cerebral hemorrhage with amyloidosis-Dutch type. *Neuropathology* 25:288–297.
14. Grabowski TJ, Cho HS, Vonsattel JP, Rebeck GW, Greenberg SM (2001) Novel amyloid precursor protein mutation in an Iowa family with dementia and severe cerebral amyloid angiopathy. *Ann Neurol* 49:697–705.
15. Bugiani O, et al. (2010) Hereditary cerebral hemorrhage with amyloidosis associated with the E693K mutation of APP. *Arch Neurol* 67:987–995.
16. Goate A, et al. (1991) Segregation of a missense mutation in the amyloid precursor protein gene with familial Alzheimer's disease. *Nature* 349:704–706.
17. Mullan M, et al. (1992) A pathogenic mutation for probable Alzheimer's disease in the APP gene at the N-terminus of beta-amyloid. *Nat Genet* 1:345–347.
18. Van Broeckhoven C, et al. (1992) Mapping of a gene predisposing to early-onset Alzheimer's disease to chromosome 14q24.3. *Nat Genet* 2:335–339.
19. Cruts M, et al. (1998) Estimation of the genetic contribution of presenilin-1 and -2 mutations in a population-based study of presenile Alzheimer disease. *Hum Mol Genet* 7:43–51.
20. Levy-Lahad E, et al. (1995) A familial Alzheimer's disease locus on chromosome 1. *Science* 269:970–973.
21. Borchelt DR, et al. (1996) Familial Alzheimer's disease-linked presenilin 1 variants elevate Abeta1-42/1-40 ratio in vitro and in vivo. *Neuron* 17:1005–1013.
22. Xia W, et al. (1997) Enhanced production and oligomerization of the 42-residue amyloid beta-protein by Chinese hamster ovary cells stably expressing mutant presenilins. *J Biol Chem* 272:7977–7982.
23. Tarasoff-Conway JM, et al. (2015) Clearance systems in the brain-implications for Alzheimer disease. *Nat Rev Neurol* 11:457–470.
24. Weller RO, Subash M, Preston SD, Mazanti I, Carare RO (2008) Perivascular drainage of amyloid-beta peptides from the brain and its failure in cerebral amyloid angiopathy and Alzheimer's disease. *Brain Pathol* 18:253–266.
25. Hawkes CA, et al. (2011) Perivascular drainage of solutes is impaired in the ageing mouse brain and in the presence of cerebral amyloid angiopathy. *Acta Neuropathol* 121:431–443.
26. Hawkes CA, et al. (2012) Disruption of arterial perivascular drainage of amyloid-β from the brains of mice expressing the human APOE ε4 allele. *PLoS One* 7:e41636.
27. Hawkes CA, Gentleman SM, Nicoll JA, Carare RO (2015) Prenatal high-fat diet alters the cerebrovasculature and clearance of β-amyloid in adult offspring. *J Pathol* 235:619–631.
28. Jenne DE, et al. (1991) Clusterin (complement lysis inhibitor) forms a high density lipoprotein complex with apolipoprotein A-I in human plasma. *J Biol Chem* 266:11030–11036.
29. de Silva HV, Harmony JA, Stuart WD, Gil CM, Robbins J (1990) Apolipoprotein J: Structure and tissue distribution. *Biochemistry* 29:5380–5389.
30. de Silva HV, et al. (1990) A 70-kDa apolipoprotein designated ApoJ is a marker for subclasses of human plasma high density lipoproteins. *J Biol Chem* 265:13240–13247.
31. Jenne DE, Tschopp J (1992) Clusterin: The intriguing guises of a widely expressed glycoprotein. *Trends Biochem Sci* 17:154–159.
32. Hermo L, Barin K, Oko R (1994) Developmental expression of sulfated glycoprotein-2 in the epididymis of the rat. *Anat Rec* 240:327–344.
33. Silkensen JR, et al. (1995) Clusterin promotes the aggregation and adhesion of renal porcine epithelial cells. *J Clin Invest* 96:2646–2653.
34. Purrello M, et al. (1991) The gene for SP-40,40, human homolog of rat sulfated glycoprotein 2, rat clusterin, and rat testosterone-repressed prostate message 2, maps to chromosome 8. *Genomics* 10:151–156.
35. Wong P, et al. (1994) Molecular characterization of human TRPM-2/clusterin, a gene associated with sperm maturation, apoptosis and neurodegeneration. *Eur J Biochem* 221:917–925.
36. Kirszbaum L, Bozas SE, Walker ID (1992) SP-40,40, a protein involved in the control of the complement pathway, possesses a unique array of disulphide bridges. *FEBS Lett* 297:70–76.
37. Wilson MR, Easterbrook-Smith SB (2000) Clusterin is a secreted mammalian chaperone. *Trends Biochem Sci* 25:95–98.

38. Bartl MM, Luckenbach T, Bergner O, Ullrich O, Koch-Brandt C (2001) Multiple receptors mediate apoJ-dependent clearance of cellular debris into nonprofessional phagocytes. *Exp Cell Res* 271:130–141.
39. Wyatt AR, et al. (2011) Clusterin facilitates in vivo clearance of extracellular misfolded proteins. *Cell Mol Life Sci* 68:3919–3931.
40. Leskov KS, Klokov DY, Li J, Kinsella TJ, Boothman DA (2003) Synthesis and functional analyses of nuclear clusterin, a cell death protein. *J Biol Chem* 278:11590–11600.
41. Yang CR, et al. (2000) Nuclear clusterin/XIP8, an X-ray–induced Ku70-binding protein that signals cell death. *Proc Natl Acad Sci USA* 97:5907–5912.
42. Aronow BJ, Lund SD, Brown TL, Harmony JA, Witte DP (1993) Apolipoprotein J expression at fluid-tissue interfaces: Potential role in barrier cytoprotection. *Proc Natl Acad Sci USA* 90:725–729.
43. Verbrugghe P, Kujala P, Waelput W, Peters PJ, Cuvelier CA (2008) Clusterin in human gut-associated lymphoid tissue, tonsils, and adenoids: Localization to M cells and follicular dendritic cells. *Histochem Cell Biol* 129:311–320.
44. Shin JK, et al. (2008) Expression of clusterin in normal and preeclamptic placentas. *J Obstet Gynaecol Res* 34:473–479.
45. Danik M, Chabot JG, Hassan-Gonzalez D, Suh M, Quirion R (1993) Localization of sulfated glycoprotein-2/clusterin mRNA in the rat brain by in situ hybridization. *J Comp Neurol* 334:209–227.
46. O'Bryan MK, Cheema SS, Bartlett PF, Murphy BF, Pearse MJ (1993) Clusterin levels increase during neuronal development. *J Neurobiol* 24:421–432.
47. Pasinetti GM, Johnson SA, Oda T, Rozovsky I, Finch CE (1994) Clusterin (SGP-2): A multifunctional glycoprotein with regional expression in astrocytes and neurons of the adult rat brain. *J Comp Neurol* 339:387–400.
48. Corder EH, et al. (1993) Gene dose of apolipoprotein E type 4 allele and the risk of Alzheimer's disease in late onset families. *Science* 261:921–923.
49. Greenberg SM, et al. (1996) Apolipoprotein E epsilon 4 is associated with the presence and earlier onset of hemorrhage in cerebral amyloid angiopathy. *Stroke* 27:1333–1337.
50. May PC, Finch CE (1992) Sulfated glycoprotein 2: New relationships of this multifunctional protein to neurodegeneration. *Trends Neurosci* 15:391–396.
51. May PC, et al. (1990) Dynamics of gene expression for a hippocampal glycoprotein elevated in Alzheimer's disease and in response to experimental lesions in rat. *Neuron* 5:831–839.
52. Matsubara E, Frangione B, Ghiso J (1995) Characterization of apolipoprotein J-Alzheimer's A beta interaction. *J Biol Chem* 270:7563–7567.
53. Oda T, et al. (1995) Clusterin (apoJ) alters the aggregation of amyloid beta-peptide (A beta 1-42) and forms slowly sedimenting A beta complexes that cause oxidative stress. *Exp Neurol* 136:22–31.
54. Matsubara E, Soto C, Governale S, Frangione B, Ghiso J (1996) Apolipoprotein J and Alzheimer's amyloid beta solubility. *Biochem J* 316:671–679.
55. DeMattos RB, et al. (2004) ApoE and clusterin cooperatively suppress Abeta levels and deposition: Evidence that ApoE regulates extracellular Abeta metabolism in vivo. *Neuron* 41:193–202.
56. DeMattos RB, et al. (2002) Clusterin promotes amyloid plaque formation and is critical for neuritic toxicity in a mouse model of Alzheimer's disease. *Proc Natl Acad Sci USA* 99:10843–10848.
57. Bell RD, et al. (2007) Transport pathways for clearance of human Alzheimer's amyloid beta-peptide and apolipoproteins E and J in the mouse central nervous system. *J Cereb Blood Flow Metab* 27:909–918.
58. Zlokovic BV, et al. (1994) Brain uptake of circulating apolipoproteins J and E complexed to Alzheimer's amyloid beta. *Biochem Biophys Res Commun* 205:1431–1437.
59. Zlokovic BV, et al. (1996) Glycoprotein 330/megalin: Probable role in receptor-mediated transport of apolipoprotein J alone and in a complex with Alzheimer disease amyloid beta at the blood-brain and blood-cerebrospinal fluid barriers. *Proc Natl Acad Sci USA* 93:4229–4234.
60. Harold D, et al. (2009) Genome-wide association study identifies variants at CLU and PICALM associated with Alzheimer's disease. *Nat Genet* 41:1088–1093.
61. Lambert JC, et al.; European Alzheimer's Disease Initiative Investigators (2009) Genome-wide association study identifies variants at CLU and CR1 associated with Alzheimer's disease. *Nat Genet* 41:1094–1099.
62. Carrasquillo MM, et al. (2010) Replication of CLU, CR1, and PICALM associations with Alzheimer disease. *Arch Neurol* 67:961–964.
63. Corneveaux JJ, et al. (2010) Association of CR1, CLU and PICALM with Alzheimer's disease in a cohort of clinically characterized and neuropathologically verified individuals. *Hum Mol Genet* 19:3295–3301.
64. Bettens K, et al. (2012) Both common variations and rare non-synonymous substitutions and small insertion/deletions in CLU are associated with increased Alzheimer risk. *Mol Neurodegener* 7:3.
65. Jankowsky JL, et al. (2004) Mutant presenilins specifically elevate the levels of the 42 residue beta-amyloid peptide in vivo: Evidence for augmentation of a 42-specific gamma secretase. *Hum Mol Genet* 13:159–170.
66. Weekman EM, et al. (2016) Reduced efficacy of anti-Aβ immunotherapy in a mouse model of amyloid deposition and vascular cognitive impairment comorbidity. *J Neurosci* 36:9896–9907.
67. Kinnecom C, et al. (2007) Course of cerebral amyloid angiopathy-related inflammation. *Neurology* 68:1411–1416.
68. Wyss-Coray T, et al. (2001) TGF-beta1 promotes microglial amyloid-beta clearance and reduces plaque burden in transgenic mice. *Nat Med* 7:612–618.
69. Cirrito JR, et al. (2003) In vivo assessment of brain interstitial fluid with microdialysis reveals plaque-associated changes in amyloid-beta metabolism and half-life. *J Neurosci* 23:8844–8853.
70. Suzuki N, et al. (1994) High tissue content of soluble beta 1-40 is linked to cerebral amyloid angiopathy. *Am J Pathol* 145:452–460.
71. Alonzo NC, Hyman BT, Rebeck GW, Greenberg SM (1998) Progression of cerebral amyloid angiopathy: Accumulation of amyloid-beta40 in affected vessels. *J Neuropathol Exp Neurol* 57:353–359.
72. Jarrett JT, Berger EP, Lansbury PT, Jr (1993) The carboxy terminus of the beta amyloid protein is critical for the seeding of amyloid formation: Implications for the pathogenesis of Alzheimer's disease. *Biochemistry* 32:4693–4697.
73. Walsh DM, Lomakin A, Benedek GB, Condron MM, Teplow DB (1997) Amyloid beta-protein fibrillogenesis. Detection of a protofibrillar intermediate. *J Biol Chem* 272: 22364–22372.
74. Fryer JD, et al. (2005) Human apolipoprotein E4 alters the amyloid-beta 40:42 ratio and promotes the formation of cerebral amyloid angiopathy in an amyloid precursor protein transgenic model. *J Neurosci* 25:2803–2810.
75. Herzig MC, Van Nostrand WE, Jucker M (2006) Mechanism of cerebral beta-amyloid angiopathy: Murine and cellular models. *Brain Pathol* 16:40–54.
76. Fryer JD, et al. (2003) Apolipoprotein E markedly facilitates age-dependent cerebral amyloid angiopathy and spontaneous hemorrhage in amyloid precursor protein transgenic mice. *J Neurosci* 23:7889–7896.
77. Herzig MC, et al. (2004) Abeta is targeted to the vasculature in a mouse model of hereditary cerebral hemorrhage with amyloidosis. *Nat Neurosci* 7:954–960.
78. Hsiao K, et al. (1996) Correlative memory deficits, Abeta elevation, and amyloid plaques in transgenic mice. *Science* 274:99–102.
79. Bu G (2009) Apolipoprotein E and its receptors in Alzheimer's disease: Pathways, pathogenesis and therapy. *Nat Rev Neurosci* 10:333–344.
80. Wyss-Coray T, et al. (2003) Adult mouse astrocytes degrade amyloid-beta in vitro and in situ. *Nat Med* 9:453–457.
81. El Khoury J, Luster AD (2008) Mechanisms of microglia accumulation in Alzheimer's disease: Therapeutic implications. *Trends Pharmacol Sci* 29:626–632.
82. Weller RO, et al. (1998) Cerebral amyloid angiopathy: Amyloid beta accumulates in putative interstitial fluid drainage pathways in Alzheimer's disease. *Am J Pathol* 153:725–733.
83. Revesz T, et al. (2003) Cerebral amyloid angiopathies: A pathologic, biochemical, and genetic view. *J Neuropathol Exp Neurol* 62:885–898.
84. Deane R, et al. (2004) LRP/amyloid beta-peptide interaction mediates differential brain efflux of Abeta isoforms. *Neuron* 43:333–344.
85. Manousopoulou A, et al. (2016) Systems proteomic analysis reveals that clusterin and tissue inhibitor of metalloproteinases 3 increase in leptomeningeal arteries affected by cerebral amyloid angiopathy. *Neuropathol Appl Neurobiol*, 10.1111/nan.12342.
86. Vinters HV, et al. (1998) Secondary microvascular degeneration in amyloid angiopathy of patients with hereditary cerebral hemorrhage with amyloidosis, Dutch type (HCHWA-D). *Acta Neuropathol* 95:235–244.
87. Wattendorff AR, Frangione B, Luyendijk W, Bots GT (1995) Hereditary cerebral haemorrhage with amyloidosis, Dutch type (HCHWA-D): Clinicopathological studies. *J Neurol Neurosurg Psychiatry* 58:699–705.
88. Maeda A, et al. (1993) Computer-assisted three-dimensional image analysis of cerebral amyloid angiopathy. *Stroke* 24:1857–1864.
89. Winkler DT, et al. (2001) Spontaneous hemorrhagic stroke in a mouse model of cerebral amyloid angiopathy. *J Neurosci* 21:1619–1627.
90. Davis J, et al. (2006) Deficient cerebral clearance of vasculotropic mutant Dutch/Iowa Double A beta in human A betaPP transgenic mice. *Neurobiol Aging* 27:946–954.
91. Eng JA, Frosch MP, Choi K, Rebeck GW, Greenberg SM (2004) Clinical manifestations of cerebral amyloid angiopathy-related inflammation. *Ann Neurol* 55:250–256.
92. Miao J, et al. (2005) Cerebral microvascular amyloid beta protein deposition induces vascular degeneration and neuroinflammation in transgenic mice expressing human vasculotropic mutant amyloid beta precursor protein. *Am J Pathol* 167:505–515.
93. National Research Council (2011) *Guide for the Care and Use of Laboratory Animals* (National Academies Press, Washington, DC), 8th Ed.
94. Liu CC, et al. (2016) Neuronal heparan sulfates promote amyloid pathology by modulating brain amyloid-β clearance and aggregation in Alzheimer's disease. *Sci Transl Med* 8:332ra44.
95. Condello C, Schain A, Grutzendler J (2011) Multicolor time-stamp reveals the dynamics and toxicity of amyloid deposition. *Sci Rep* 1:19.